FRAMEWORK OF HYBRID RENEWABLE ENERGY WITH CONVENTIONAL POWER GENERATION SCHEDULING USING NOVEL METAHEURISTIC OPTIMIZATION ALGORITHM

Kingsuk Majumdar,* Provas K. Roy,** and Subrata Banerjee*

Abstract

In the present era, only thermal generation cannot be a solution to modern demand. The hybrid renewable energy with conventional power generation is the answer to save mother nature and meet the current electricity demand. In this article, traditional thermal power plants are interconnected with natural resources like wind, hydro units with all-day planning and operation strategies. And the generated power is needed to transfer from one section to another section in the existing grid system, which is the subject of available transfer capability (ATC), the modern power system's critical factor. In this article, the minimization of power generation cost of the thermal power units is achieved by incorporating renewable sources, says hydro, and wind plants for 24 h scheduled, and ATC calculation is the prime objective. In recent literature, the mayfly algorithm (MA) optimization approach, which combines the advantages of evolutionary algorithms and swarms intelligence to attend better results, is successfully implemented. In this article, optimum power flow (OPF)-based ATC is enforced under various conditions with hydro–thermal–wind scheduling concept on the IEEE 39-test bus system to check the proposed chaotic MA's performance. The chaotic MA (CHMA) is a hybridized format of the MA and chaotic map method. It is noted from the simulation study that the suggested novel CHMA approach has a dominant nature over other well-established optimization algorithms. Also in the case of multi-objective function, the cost function value is improved by more than 10% and ATC value is enhanced by near about 60% and more.

* Department of Electrical Engineering, National Institute of Technology, Durgapur, Durgapur, West Bengal, 713209, India; e-mail: kingsuk.majumdar5@gmail.com, bansub2004@yahoo.com

** Department of Electrical Engineering, Kalyani Government Engineering College, Kalyani, West Bengal, India; e-mail: roy_provas@yahoo.com

Corresponding author: Kingsuk Majumdar

Recommended by Prof. Yao Xu
(DOI: 10.2316/J.2022.203-0387)

Key Words

Available transfer capability (ATC), Chaotic Mayfly algorithm (CHMA), Hydro-thermal-wind scheduling (HTW), Mayfly algorithm (MA), Optimum power flow (OPF)

1. Introduction

In the present era, to save mother nature and reduce the thermal power plant's generation cost, natural resources are involved. In this article, hydro and wind power plants are incorporated with conventional thermal units to achieve the goal. The authors have also done 24 h load-scheduling and popper coordination of all the said natural resources with thermal units to match the load demand. The North American Electric Reliability Council defines available transfer capability (ATC) as the amount of extra transportable power through the existing transmission system without violating power system constraints. As per the guideline of Federal Energy Regulatory Commission, the basic ATC data must be available on an hourly basis in an open-access market. The distribution generations (DGs) add up to the complexity of the modern power system framework. It is to enhance the capacity of transferring electrical power in the existing network for future transaction to deal with contingencies and uncertainties of the power system [1]. In the present era, with the rising economy, power transfers have been enhancing at a much higher rate than transmission capacity, which abbreviated reliability and system security. ATC assessment is the window to provide adequate knowledge in advance on these types of power transactions through the existing electrical power network without violating the power system constraints [1]–[3].

Estimating any parameter in real-time adds an extra hurdles to its evaluation process like ATC calculation. This real-time ATC evaluation gives ample benefits in financial and engineering aspects as follows:

1. If the ATC knowledge is known in advance, more operating windows will be opened for the operator to run the power system in 10 times or more power transaction conditions.
2. The development and implementation of natural resources like wind–hydro and the smart grid inject more uncertainties, making real-time ATC determination a hard nut to crack [2].
3. The online study can be boiled down to those cases relevant to actual operating circumstances.

In early growths of ATC, estimation depends on the network's power flow; hence, their computational speed is high. However, the modern power system consisting of a grid and large-scale distributed generators (DGs) make electrical power flow equations complex and non-linear in nature. Therefore, to estimate the value of ATC by most of the linearized methods cannot be implemented easily, as it involves voltage stability, thermal limit, reactive power generation limit and other power system constraints. In the present era, several computational methods have been investigated for the same as follows:

- in view of optimum power flow (OPF) approach;
- as a distributed state estimation process;
- with the concept of distributed control for distribution networks;
- conceding voltage stability monitoring [4];
- with distributed contingency analysis method [5];

Particle swarm optimization (PSO), grey wolf optimizer (GWO) and mayfly algorithm (MA) and chaotic MA (CHMA) optimization are incorporated with the OPF concept to achieve accurate estimation of ATC without violating power system constraint parameters. This article aims to furnish the estimated ATC by subdividing it into some zone of areas and, more preciously say, using tie-line. Therefore, the ATC estimation can be formulated as a distributed multi-area OPF problem by considering both inequality and equality criteria. Due to the enormous development of computational power in modern days, computation time and memory complexity are no longer a great deal. By proper coordinated and distributed mechanism, the ATC of the entire power grid can be obtained in real-time. In brief, the prime objectives of this article can be enlisted as follows:

1. The thermal–hydro–wind scheduling along with variation of demands for 24 h is taken into consideration during the problem formulation in this article.
2. To reduce the cost of generation and to save the environment, thermal power plants are coordinated with hydro–wind units.
3. Generally, ATC is calculated without considering the generation cost. In this article, generation cost is also taken into consideration, which makes the said problem multi-objective optimization.
4. The multi-objective ATC problem is formulated using OPF concept along with multi-objective MA algorithms.

The rest of this article is organized as follows: In Section 2, the mathematical modelling is fabricated, as mentioned earlier, associated with the thermal unit and other natural energy sources like wind and hydro. In the following section, proposed single and multi-objective MA optimization is described vividly. Afterwards, the application of the mechanism as mentioned earlier has been studied for standard IEEE 39-bus system under different test cases in Section 4. Finally, the future scope and conclusion have been discoursed in Section 5.

2. Mathematical Modelling of the System

In this mathematical modelling section, the active power generation with 24 h scheduling and ATC estimation has been done step by step. This scheduling has machinated in coordination among thermal, wind and hydro plants.

2.1 Wind Power Generation and Its Generation Cost

The generation of wind energy from wind is uncertain due to the variation in wind speed. The wind speed can be predicted using probability density function (1) as follows:

$$pdw(S_{1h}, S_{1f}, vl) = \exp\left(-\left(\frac{vl1}{S_{1f}}\right)^{S_{1h}}\right) * \frac{S_{1h}}{S_{1f}}\left(\frac{vl1}{S_{1f}}\right)^{S_{1h}-1} \quad (1)$$

The cumulative density function (cdf) termed as *pdw* for the wind speed can be expressed as follows (2):

$$cdw(S_{1h}, S_{1f}, vl1) = 1 - \exp\left[-\left(\frac{vl1}{S_{1f}}\right)^{S_{1h}}\right] \quad (2)$$

The relation between wind velocity and wind power is represented by a linear model as the generation of wind power depends on the velocity of the wind (3)

$$wnd = \begin{Bmatrix} wnd_{1R};\ vl_{1R} \le vl \le vl_{1out} \\ 0;\ vl < vl_{1in} \text{ or } vl \ge vl_{1out} \\ \dfrac{wnd\,(vl - vl_{1in})}{vl_{1R} - vl_{1in}};\ vl_{1in} \le vl \le vl_{1out} \end{Bmatrix} \quad (3)$$

Using (4) and (5), the authors have calculated the probability of wind power as *wnd* and zero wind condition as

$$P_{wnd}\,(wnd = 0) = cdw\,(vl_{1in}) - (cdw\,(vl_{1out}) - 1) = 1 + \exp\left(-\left(\frac{vl_{1out}}{S_{1f}}\right)^{S_{1h}}\right) - \exp\left(-\left(\frac{v1l_{in}}{S_{1f}}\right)^{S_{1h}}\right) \quad (4)$$

$$P_{1wnd}\,(wnd = wnd_{1R}) = cdw\,(vl_{1out}) - (cdw\,(vl_{1R}) - 1) = \exp\left(-\left(\frac{vl_{1out}}{S_{1f}}\right)^{S_{1h}}\right) - \exp\left(-\left(\frac{vl_{1in}}{S_{1f}}\right)^{S_{1h}}\right) \quad (5)$$

where cfw of the random variable (wnd) by considering (4) and (5) can be written as follows:

$$f_{wnd}(1wnd) = \begin{cases} 1; wnd > wnd_{1R} \\ 0; wnd < 0 \\ \begin{cases} \frac{Vl_{1in} S_h H_{wnd}}{Wnd_R S_f} \left(\frac{(wnd_{1R} + H_{1wnd}) Vl_{1in}}{wnd_{1R} S_{1f}} \right) \\ \times \exp\left(- \frac{(wnd_{1R} + H_{1wnd}) Vl_{1in}}{wnd_{1R} S_{1f}} \right); \\ 0 < wnd \leq wnd_{1R} \end{cases} \end{cases} \tag{6}$$

where

$$H_{1wnd} = -1 + \left(\frac{vl_{1R}}{vl_{1in}} \right) \tag{7}$$

Wind power production is not steady due to wind speed; hence, wind power is sometimes less than the demand (overestimated scenario) or more than load demand (underestimated scenario). Two additional cost terms are involved: overestimation and underestimation cost, respectively, and are joined to both cases of wind power generation. The underestimation and overestimation cost formulas can be jotted as follows:

$$\begin{aligned} E_{1wnd,1Z,1T} = C_{1wnd,1Z}(wnd_{1R,1Z} - wnd_{1Z,1T}) \left\{ \exp\left(- \left(\frac{Vl_{1in,1Z}}{S_{1f,1Z}} \right)^{S_{1h,1Z}} \right) - \exp\left(- \left(\frac{Vl_{1out,Z}1}{S_{1f,1Z}} \right)^{S_{1h,1Z}} \right) \right\} \\ + \left\{ \exp\left(- \left(\frac{Vl_{1in,1Z}}{S_{1f,1Z}} \right)^{S_{1h,1Z}} \right) - \exp\left(- \left(\frac{Vl_{1in,1Z}}{S_{1f,1Z}} \right)^{S_{1h,1Z}} \right) \right\} \left\{ wnd_{1Z,1T} + \frac{wnd_{1R,1Z} Vl_{1in,1Z}}{v_{1in,1Z} - v_{1out,1Z}} \right\} \\ + \left\{ \Gamma \left\{ \left(\frac{1}{S_{1h,1Z}} \left(\frac{Vl_{1in}}{S_{1f,1Z}} \right)^{S_{1h,1Z}} \right) + 1 \right\} + \Gamma \left\{ \left(\frac{1}{S_{1h,1Z}} \left(\frac{Vl_{1R,1Z}}{S_{1f,1Z}} \right)^{S_{1h,1Z}} \right) + 1 \right\} \right\} \frac{wnd_{1R,1Z} S_{1f,1Z}}{Vl_{1R,1Z} - Vl_{1in,1Z}} \end{aligned} \tag{8}$$

To match the demand, it is required to purchase the power from the wind farm operator which is called direct cost of wind power and it can be formulated as follows (9):

$$E_{dr.1Z.1T} = wnd_{1Z.1T} \times g_{1Z} \tag{9}$$

Therefore, the wind power generation considering under and overestimation and direct cost of wind generation for each interval are as follows (10):

$$E_{wnd\_tot} = \sum_{1Z=1}^{N_{1wnd}} \sum_{t=1}^{1T_{hor}} (E_{dr.1Z.1t} + E_{UN.1Z.1t} + E_{1OVR.1Z.1t}) \tag{10}$$

where N_{1wnd} is the total number of wind generators.

2.2 Hydro-Power Generation and Its Generation Cost

The running cost of a hydro-power generation unit is negligible as it is very low. Hence, hydro-power generation unit can be combined with thermal power plant to reduce its fuel and emission cost [6]. The hydro-power generation $PHY_{i,t}$ is related to discharge rate of water and storage volume and can be formulated as follows:

$$\begin{aligned} PHY_{i,1t} = CHi_{6,1t} + CHi_{5,1t} disq_{i,1t} + CHi_{4,1t} Vol_{i,1t} \\ + CHi_{3,1t} disq_{i,1t} Vol_{i,1t} + CHi_{2,1t} Vol_{i,1t}^2 \\ + CHi_{1,1t} disq_{i,1t}^2 \end{aligned} \tag{11}$$

where $CHi_{1,1t}$, $CHi_{2,1t}$, $CHi_{3,1t}$, $CHi_{4,1t}$, $CHi_{5,1t}$ and $CHi_{6,1t}$ are coefficients of the hydro generation unit; $Vol_{i,t}$ and $disq_{i,1t}$ are volume of water of i^{th} units and discharge rate of i^{th} unit, respectively.

2.3 Thermal Power Generation and Its Generation Cost

Thermal power generator is generally represented with valve point effect along with quadratic function [7], [8] as shown below:

$$\begin{aligned} F_{Th\_tot} = \sum_{t=1}^{T} \sum_{i=1}^{N_{genTH}} (\alpha_i P_{th_i}^2 + \beta_i P_{th_i} + \gamma_i \\ + \mid e_{1_i} \sin(e_{2_i}(-P_{thmin_i} + P_{th_i})) \mid) \end{aligned} \tag{12}$$

where, α_i, β_i, γ_i are the fuel coefficients and e_{1_i}, e_{2_i} are the valve point loading effect constant and P_{thmin_i} is the minimum active power generation of the i^{th} thermal unit [9]. The total number of thermal generator is N_{genTH}.

Therefore, the active power generation cost for thermal unit along with wind and hydro unit can be formulated as follows:

$$F_{gen\_tot} = E_{wnd\_tot} + F_{Th\_tot} + \gamma_w \sum_{t}^{H} \sum_{i=1}^{N_{genHY}} PHY_{i,t} \tag{13}$$

where γ_w is a scalar constant which converts water volume discharge to equivalent generation cost.

2.4 Problem Formulation of Available Transfer Capability Along with Hydro–Thermal–Wind Scheduling

In this article, the OPF concept is employed to face the challenges of ATC. The cost function, *i.e.*, the objective function, is originated at possible maximum power flow from a particular zone of generating units in a source area to the load buses in a sink area through some specific transmission or tie-lines without assaulting the power system

operation constraints and limits. The thermal limit of a line is taken as an upper limit of the particular line's power transaction. The cost function for ATC based on OPF is formulated mathematically. Generally, for ATC problem, active power generation cost is not considered, but here both ATC and power generation cost are considered. In this article, mainly two different cases are considered as follows:

- CASE A: Minimization of active power generation cost alone (using HTW scheduling) [10], [11]
- CASE B: Maximization of ATC along with minimization of active power generation cost with renewable energy sources (multi-objective)[12].

Therefore, the cost function can be formulated as follows:

$$F_{Tot} = \psi_{TL}F_{TL} + \psi_{TLA}F_{TLA} + \psi_V F_{Vmis} + \psi_{gen}F_{gen\_tot} \tag{14}$$

where ψ_{TL}, ψ_V, ψ_{TLA} and ψ_{gen} are different positive scalar values for the objective function. Given suitable weight, on these scalar factors, single or/and multi-objection cost function can be achieved. For enhancement of ATC, power flow should be raised through some particular lines and can be shown as:

$$F_{TLA} = \left| \left(\frac{1}{S_{TLi} - S_{TLBi}} \right) \right| \tag{15}$$

where S_{TLi} and S_{TLBi} are power flow through the ith line and base power flow through the line, respectively. To confine overloading of transmission line, a mathematical factor is introduced in the cost function as follows:

$$F_{TL} = \sum_{i=1}^{NTL} \left(S_{TL\max_i} - S_{TL_i}\right)^2 \quad if S_{TL\max_i} < S_{TL_i} \tag{16}$$

The equality constraints of the load flow are as follows:

$$P_{G_i} - P_{D_i} - \sum_{j=1}^{NBUS} V_i Y_{ij} V_j \cos\left(\theta_{ij} + \delta_j - \delta_i\right) = 0 \tag{17}$$

$$Q_{G_i} - Q_{D_i} + \sum_{j=1}^{NBUS} V_i Y_{ij} V_j \sin\left(\theta_{ij} + \delta_j - \delta_i\right) = 0 \tag{18}$$

The voltage, active power and reactive power generation constraints are as follows:

$$V_i^{\min} \le V_i \le V_i^{\max}; i = 1, ..., NBUS \tag{19}$$

$$P_{Gi}^{\min} \le P_{G_i} \le P_{Gi}^{\max}; i = 1, ..., NGEN \tag{20}$$

$$Q_{Gi}^{\min} \le Q_{G_i} \le Q_{Gi}^{\max}; i = 1, ..., NGEN \tag{21}$$

where $NBUS, NGEN$ are total number of bus and generator bus, respectively, and $V_i^{\max}, P_{Gi}^{\max}, Q_{Gi}^{\max}$ and $V_i^{\min}, P_{Gi}^{\min}, Q_{Gi}^{\min}$ are maximum and minimum voltages, active and reactive power generation limits, respectively, in the IEEE test system.

The shunt reactor compensations and tap setting transformer of the test system can be represented, respectively, as follows:

$$Q_{SHi}^{\min} \le Q_{SHi} \le Q_{SHi}^{\max}; i = 1, ..., NSH \tag{22}$$

$$T_i^{\min} \le T_i \le T_i^{\max}; i = 1, ..., NT \tag{23}$$

Table 1
Value of Different Cost Scalar Factors at Different Cases

Case	ψ_{TL}	ψ_V	ψ_{TLA}	ψ_{gen}
Case A	1,000	1,000	0	1
Case B	20	20	10	0.001

where NSH, NT are total number of shunt reactors and tap-transformers and super subscript min and max are their minimum and maximum values, respectively. The scalar constants in (14) have different value at different case conditions and are tabulated in Table 1.

3. Proposed Algorithms and Their Implementation

In this section, different types of metaheuristic algorithms [13] including the proposed multi-objective chaotic MA (CHMA) are discussed to solve the said problems.

3.1 Grey Wolf Optimizer Algorithm and Its Implementation

The GWO is at first brought in by Mirjalili *et al.*, in 2014 [14], [15]. The algorithm deals with the hunting mechanism and democratic behaviour of grey wolves in a pack in nature. In a pack, a very strict social dominant hierarchy is followed by the grey wolf. The social dominant hierarchy and algorithm are well described in the aforesaid literature.

3.2 The Proposed Mayfly Algorithm

Mayflies [16] are part of an ancient group of insects called Palaeoptera, which are insects that belong to the order Ephemeroptera. The proposed MA optimization method is a potent hybrid algorithmic structure that is an upgradation of PSO [17] and considering the critical advantages of PSO, GA [18] and MA. The social behaviour of mayflies, especially their mating process, is the backbone of the proposed algorithm. It is assumed that mayflies are already adults and the fittest mayflies survive after hatching from the egg, irrespective of how long they live. The position of each mayfly in the search space represents a potential solution to the proposed problem. The algorithm works as follows. Initially, two sets of mayflies are randomly generated, representing the male and female populations, respectively. In the said algorithm, each mayfly is randomly located in the N-dimensional problem search space as a candidate solution, represented as a vector $x_i = (x_{i_1}, x_{i_2}, ..., x_{i_N})$ and $y_i = (y_{i_1}, y_{i_2}, ..., y_{i_N})$ for male and female mayfly, respectively. The velocity of the same is presented by $v_i = v_{i_1}, v_{i_2}, ..., v_{i_N}$. The direction of movement and trajectory of each mayfly is influenced by individual best (P_{ibest}) and global best (g_{best}).

3.2.1 Movement of Male Mayflies

Males are gathering in swarms implies that each male mayfly's position adjusted according to both its own ex-

perience and that of its neighbours. The current position ($x_j^{t_0+1}$) and velocity ($v_{ji}^{t_0+1}$) of the j^{th} mayfly are represented, respectively, as follows:

$$x_j^{t_0+1} = v_j i^{t_0+1} + x_j^{t_0} \tag{24}$$

$$v_j i^{t_0+1} = v_j i^{t_0} + A(pbest_{ji} - x_{ji}^{t_0}) + B(gbest_i - x_{ji}^{t_0}) \tag{25}$$

3.2.2 Movement of Female Mayflies

The female mayflies do not gather in a swarm-like males; instead, they fly towards males to breed. The velocity and position of the female mayfly can be represented as follows:

$$v_{ji}^{t_0+1} = \left\{ \begin{array}{l} rand(1,-1) * fl + v_{ji}^{t_0}; \text{if } f(y_j) \leq f(x_j) \\ -a_2 * exp(-\beta r^2 m_f) * (y_{ji}^{t_0} - x_{ji}^{t_0}) + v_{ji}^{t_0}; \\ \text{if } f(x_j) < f(y_j) \end{array} \right\} \tag{26}$$

where fl is a random walk coefficient, used when a female is not attracted by a male and r_{mf} is the Cartesian distance between male and female mayflies and β is a fixed visibility coefficient. Finally, rand(1, −1) gives random number in between 1 and −1.

3.2.3 Mating of Mayflies

The crossover represents the mating process between two mayflies: two different genders are taken from their population as parents. The way parents are selected is the same as males attract the females. Notably, the selection can be either based on their fitness function value or random. In the latter, the best female breeds with the best male, the second-best female with the second-best male like that. Each crossover produces two offspring and mathematically can be expressed as follows:

$$off_1 = (1 - L) * F + L * M \tag{27}$$

$$off_2 = (1 - L) * M + L * F \tag{28}$$

where L is the random value in the specific range; M, L stand for male and female parents, respectively. Finally, off_1 and off_2 are offspring whose initial velocities are set to zero. The full pseudo code of the said algorithm is shown in Algorithm 1.

3.3 Chaotic Maps

In this section, the authors have described the proposed hybrid MA algorithm that uses the chaotic scale factor concept. The primary factor and condition sensitivity are the main concerns in a chaotic system. The chaos concept has played a crucial role in the initialization process of said MA. Hence, this article gives the hybridization of chaos and MA to achieve better convergence of the problem. In general, the chaotic combinations are non-linear stimulation systems and, hence, responsiveness depends on both system parameter variations and initial expressions [19]. There are a lot of different chaotic maps that have been proposed in different literature. In this article, 10 different

Algorithm 1 MA algorithms

Cost function $f(X), X = (x_1, x_2, ...x_N)^T$;
initialization of population:
female mayfly velocity (v_{fj}) and position y_j;
male mayfly velocity (v_{mj}) and position x_j;
Evaluate candidate solutions
Calculate the pbest and gbest

while stopping condition are not met **do**
    Upgrade velocities and solutions of females and males
    Calculate solutions
    Ranking the mayflies
    Mating the mayflies
    Evaluating offspring
    Randomly, separate offspring to female and male
    Exchange worst solutions with the best new ones
    Update gbest and pbest
end while
print results

chaotic maps are taken under consideration, *i.e.*, circle, cubic, logistic, Gaussian/mouse, sinusoidal, sine, singer, tent, piece-wise and iterative [20]. As mentioned above, 10 chaotic maps are incorporated with MA algorithms during the generation of MA's initial population for the rest of the simulation study. Afterwards, the relevant chaotic map is selected to implement in the IEEE 39-bus system under different cases.

3.4 Implementation of Chaotic Mayfly Algorithm into Proposed Problem

In this section, the implementation of the proposed hybrid chaotic MA is discussed as follows:

- Step I: Randomly generate the initial population with various chaotic mapping and check for feasibility
- Step II: Evaluate position and velocity of female and male using (24), (25) and (26)
- Step III: Calculate the pbest and gbest of population
- Step IV: Ranking and evaluation of off spring is done using (27) and (28)
- Step V: Randomly separate female and male off spring
- Step VI: Exchange worst solutions with the best new ones
- Step VII: Update pbest and gbest
- Step VIII: If maximum iteration is not reached, go to Step II else next Step
- Step IX: Print all best control variables and show the convergence curve and voltage profile. It is shown in Fig. 1.

The different types of chaotic maps are used in various literature [20], say circle chaotic map, cubic chaotic map, logistic chaotic map, Gaussian/mouse chaotic map, sine chaotic map, sinusoidal chaotic map, singer chaotic map, piece-wise chaotic map, tent chaotic map, iterative chaotic map and are marked as CH1, CH2, CH10, respectively. In the algorithm mentioned above, CH10 (*i.e.*, iterative chaotic map) chaotic map can be replaced by any other one. But it is observed that CH10 is better than others concerning the said problem. Hence, it is hybridized with basic MA (CHMA10 or simply CHMA).

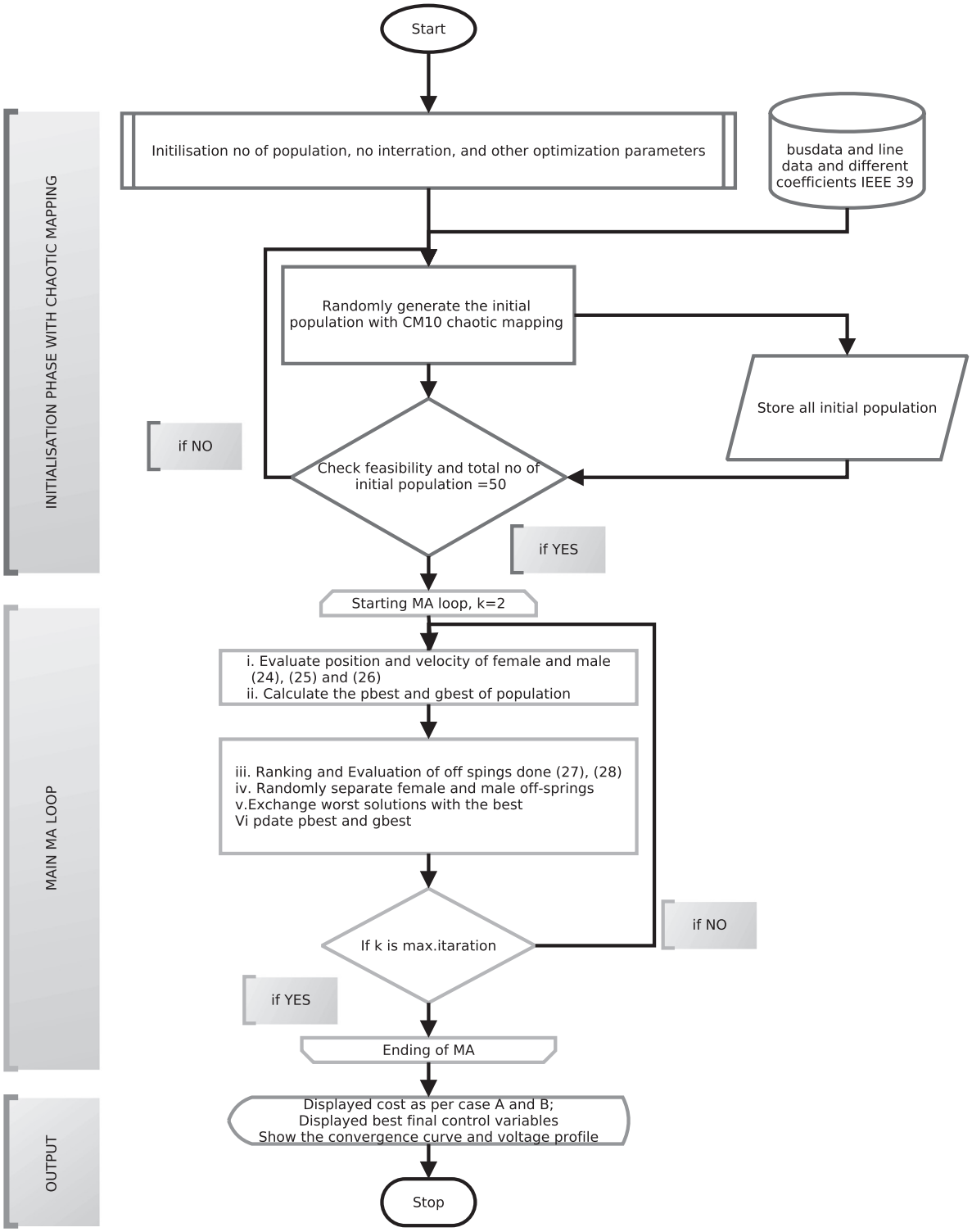

Figure 1. Flow chart of CHMA.

4. Results and Discussion

In this article, two cases (CASE A and CASE B, mentioned above) are implemented on IEEE 39-bus system, and the authors have examined the effectiveness of the proposed algorithms. The IEEE 39-bus test system data have been taken from MATPOWER tool box; each test case and each optimization are taken for 30 trial run. The initial population is taken as 50 for all individual case. All test cases have been implemented on HP system with Intel Core i3, 1.8 GHz processor, Windows 10 (home) operating system with 6 GB of DDR3 RAM memory and Matlab 2016a. In this article, the 10 different chaotic maps are implemented on 39-bus system for condition CASE A with 30 random trial runs and iterative chaotic map hybridization with MA is taken into consideration for all the cases of study.

4.1 39-bus Test System Study and Result

In the 39-bus test system, there are 39 buses, 14 numbers of generating units, among them four are hydro units, four are wind unit and six are thermal unit. There are 25 load buses having total active base load demand of 61.566 PU and total reactive base load demand of 13.429 PU, respectively, and the 24 h load demand is changed as per the H-factor shown in Table 2. Two cases are studied one after another. In the first case, the authors are focused on minimizing the generation cost only; in the second case, minimization of generation cost is given along with maximization of ATC (multi-objective), which are titled Case A and Case B, respectively. Line no. 9 *i.e.* from bus 4 to bus 14 is taken into consideration for ATC calculation in this article.

In first case, *i.e.* CASE A, the authors have focused to minimize the generation cost only. In Table 3, minimization of total cost after 30-random trial run using PSO is 355,898.7012 $/24 h, whereas MA provides 353,394.3151 $/24 h and the proposed CHMA shows 350,581.3336$/24 h. All generating bus voltage magnitudes are shown in the 3D plot in Fig. 3.

Finally, the authors have discussed about multi-objective optimization by minimization of overall cost along with ATC maximisation, *i.e.* CASE B. It is ob-

Table 2
Active and Reactive Power Demand of 39-bus System for 24 h.

Hr	H-factor	Hr	H-factor	Bus no	Base P_d	Base Q_d	Bus no	Base P_d	Base Q_d	Bus no	Base P_d	Base Q_d
1	0.438	14	0.518	1	0.0000	0.0000	14	0.0000	0.0000	27	2.8100	0.7550
2	0.422	15	0.542	2	0.0000	0.0000	15	3.2000	1.5300	28	2.0600	0.2760
3	0.394	16	0.479	3	3.2200	0.0240	16	3.2900	0.3230	29	2.8350	0.2690
4	0.315	17	0.505	4	5.0000	1.8400	17	0.0000	0.0000	30	0.0000	0.0000
5	0.434	18	0.622	5	0.0000	0.0000	18	1.5800	0.3000	31	0.0920	0.0460
6	0.413	19	0.688	6	0.0000	0.0000	19	0.0000	0.0000	32	0.0000	0.0000
7	0.457	20	0.635	7	2.3380	0.8400	20	6.8000	1.0300	33	0.0000	0.0000
8	0.510	21	0.599	8	5.2200	1.7660	21	2.7400	1.1500	34	0.0000	0.0000
9	0.500	22	0.489	9	0.0650	−0.666	22	0.0000	0.0000	35	0.0000	0.0000
10	0.494	23	0.433	10	0.0000	0.0000	23	2.4750	0.8460	36	0.0000	0.0000
11	0.484	24	0.444	11	0.0000	0.0000	24	3.0860	−0.922	37	0.0000	0.0000
12	0.524			12	0.0850	0.8800	25	2.2400	0.4720	38	0.0000	0.0000
13	0.564			13	0.0000	0.0000	26	1.3900	0.1700	39	11.0400	2.5000

Table 3
Cost Comparison of Various Methods Under Different Strategies of 39-bus System for 24-h

Methods	Mini total fitness cost	ATC (24 h)	Only gen cost	Thermal gen cost	Wind cost	Line flow violation	no of trail	Simulation time(s)
Case A: Only generation cost optimization								
PSO	355,898.7012	0.0730	355,898.7012	353,253.1463	2,645.5534	0	30	48
GWO	355,514.4792	0.0785	355,511.4663	348,705.0348	6,806.4315	0	30	42
MA	353,394.3151	0.0780	353,392.3355	347,095.1784	6,297.1571	0	30	50
CHMA	350,581.3336	0.0840	350,580.2207	347,096.0451	3,484.1756	0	30	97
Case B: Multi-objective								
PSO	543.8915	0.0580	371,477.6916	368,242.4571	3,235.2345	0	30	50
GWO	453.7226	0.1170	368,252.4908	365,130.9214	3,121.5694	0	30	49
MA	450.8046	0.1210	368,160.0211	364,990.1245	3,169.8966	0	30	65
CHMA	447.4089	0.1260	368,043.8115	364,773.2548	3,270.5567	0	30	121

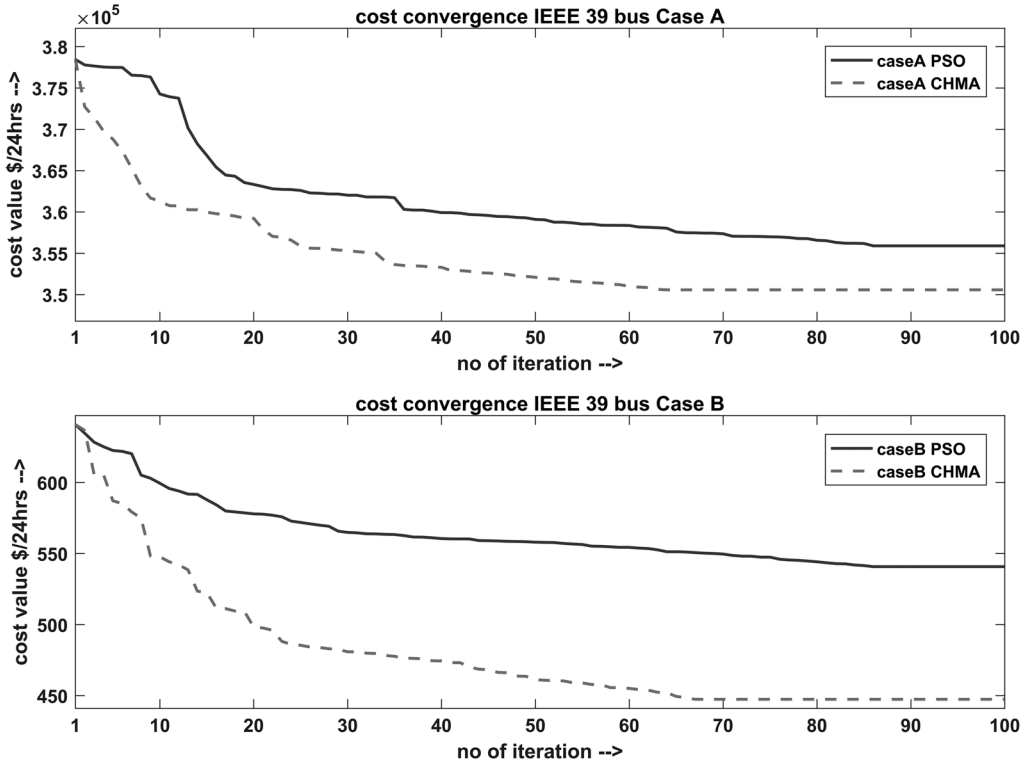

Figure 2. Cost convergence of 39-bus system under various test scenario.

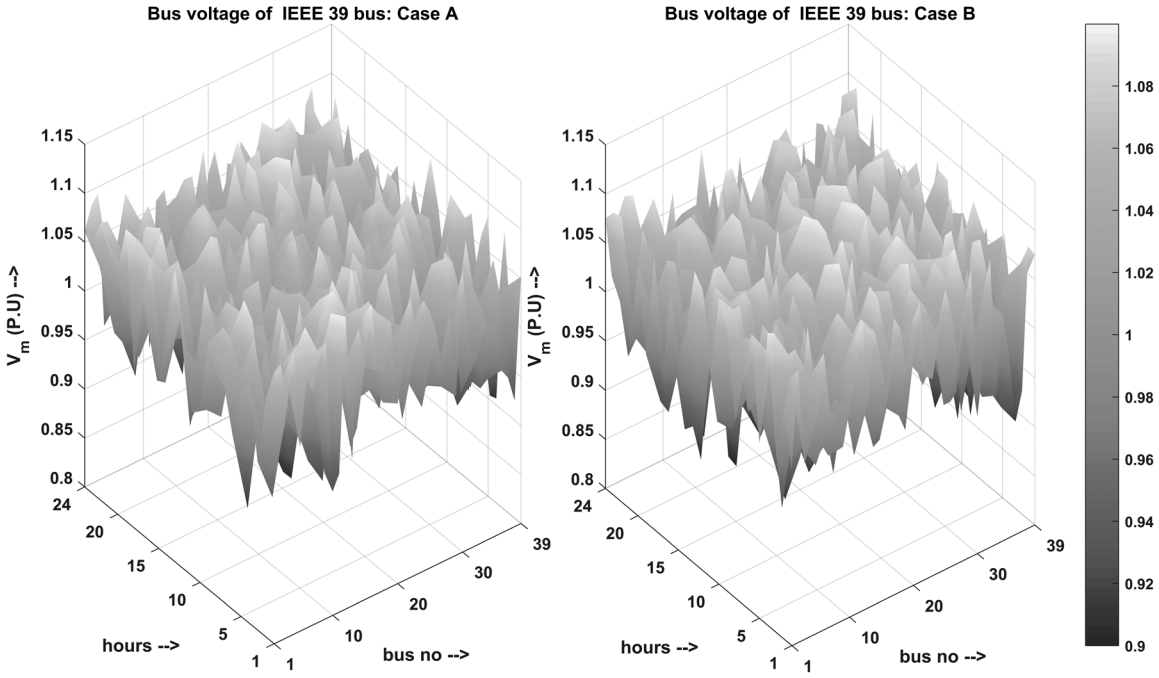

Figure 3. Voltage of various buses under various test scenario for 39-bus system.

served that again CHMA technique produces best results as 447.4089 $/24 h among other proposed algorithms considering 30 individual trial runs. From Table 3, it is observed that it is a reduction of 19.75% of the overall cost function value compared to PSO and simultaneously enhancing ATC value almost doubles as compared to PSO. The voltage profile for all buses for 24 h for all cases is described in the 3D plot in Fig. 3. The convergence curves are presented in Fig. 2, which emphasise the superiority of proposed CHMA over other methods. In Table 4, Friedman's test on IEEE 39-bus system for case B has been performed, where P_{val} is 1.62E-15, number of trial run (n) is 30 and four different types of optimizations (*i.e.*, PSO, GWO, MA, CHMA) are considered. Therefore, the dominant nature of the proposed CHMA is established. The authors have also used standard test bench functions to judge the dominating nature of CHMA over basic MA and results are tabulated in the appendix as Table A.1.

Table 4
Friedman's Test on IEEE 39-bus System for Case B

Sample	PSO	GWO	MA	CHMA		PSO	GWO	MA	CHMA
1	545.9872	474.5840	482.8606	464.0979		4	2	3	1
2	571.2458	471.5111	456.5006	448.1627		4	3	2	1
3	587.1236	459.9776	466.7811	455.1036		4	2	3	1
4	553.8978	471.4593	463.0169	455.7637		4	3	2	1
5	584.8187	456.3558	461.0587	452.8568		4	2	3	1
6	586.0333	456.6622	477.6782	453.7755		4	2	3	1
7	573.8649	501.5188	482.4823	450.1152		4	3	2	1
8	559.2365	561.3650	457.9762	450.4551		3	4	2	1
9	546.3135	459.7385	462.1481	450.4609		4	2	3	1
10	565.2354	454.7262	473.8687	453.6970		4	2	3	1
11	586.0620	458.0179	454.5128	456.2875		4	3	1	2
12	611.6132	456.8158	465.5451	452.8648		4	2	3	1
13	556.9765	467.9504	470.8029	447.5516		4	2	3	1
14	563.0816	461.3945	455.8233	459.7472		4	3	1	2
15	613.4252	489.2673	487.6916	451.8880		4	3	2	1
16	562.2238	479.9885	489.6591	454.6128		4	2	3	1
17	544.2365	565.4683	453.8268	456.4949		3	4	1	2
18	565.4427	465.7182	466.7174	450.1652		4	2	3	1
19	576.6443	473.4106	466.8889	453.6791		4	3	2	1
20	594.6196	473.6388	453.4211	449.2987		4	3	2	1
21	555.2603	467.8206	452.5669	461.2351		4	3	1	2
22	589.5663	476.6459	466.8128	451.4151		4	3	2	1
23	564.6518	468.8099	465.4084	453.6114		4	3	2	1
24	553.8834	494.3380	456.3462	451.2568		4	3	2	1
25	549.4066	471.2916	456.2280	449.8839		4	3	2	1
26	613.9891	461.3026	451.9305	454.9799		4	3	1	2
27	576.6336	477.8419	473.8422	452.9322		4	3	2	1
28	569.5212	502.2593	475.8836	449.5486		4	3	2	1
29	543.8915	453.7226	450.8046	447.4089		4	3	2	1
30	552.3915	461.0876	456.2633	449.5342		4	3	2	1
$n = 30$	$k = 4$	$Q = 71.96$	P_val = 1.62E-15< 0.05			Statistical results			
$\sum R$	118	82	65	35	Min	543.8915	453.7226	450.8046	447.4089
$\sum R^2$	13,924	6,724	4,225	1,225	Max	613.9891	565.4683	489.6591	464.0979
$\sum R_j^2$	26,098				Ave	570.5759	476.4896	465.1782	452.9628

Ranking analysis

5. Conclusion

This article introduces a recent methodology for dealing with ATC calculation and generation cost optimization incorporating renewable souses, *i.e.*, hydro and wind. The proposed method, *i.e.* CHMA method, has been verified by examining its superior convergence characteristics and higher efficiency with other metaheuristic optimizations. The uncertainties of wind power and load requirement are taken into consideration. The incorporation of wind and hydro units to the traditional thermal generating units to minimize the overall active power generation cost is another objective of this article. The results executed by the projected approach are correlated through the results established by the similar heuristic methods, say PSO, GWO, MA, revealed in the current literature. The efficiency of the proposed method is substantiated using IEEE 39-bus test systems for two different cases. In each case, the proposed method shows that convergence characteristics and computational efficiency of CHMA are superior to that of the other methods. Also to substantiate the effectiveness of CHMA-10 over basic MA, standard five test bench functions are taken and results are tabulated in the appendix section in Table A.1. This article handles the problems regarding ATC with hydro–thermal and wind scheduling for 24 h, which is the uniqueness of this article.

References

[1] A.R. Bergen, *Power systems analysis* (Pearson Education, India, 2009).

[2] G.C. Ejebe, J. Tong, J. Waight, J. Frame, X. Wang, and W. Tinney, Available transfer capability calculations, *IEEE Transactions on Power systems*, *13*(4), 1998, 1521–1527.

[3] H.-D. Chiang and H. Li, *On-line ATC evaluation for large-scale power systems: Framework and tool* (Springer, Boston, MA, 2005).

[4] L. Xie, Y. Chen, and H. Liao, Distributed online monitoring of quasi-static voltage collapse in multi-area power systems, *IEEE Transactions on Power Systems 27*(4), 2012, 2271–2279.

[5] Q. Morante, N. Ranaldo, A. Vaccaro, and E. Zimeo, Pervasive grid for large-scale power systems contingency analysis, *IEEE Transactions on Industrial Informatics*, *2*(3), 2006, 165–175.

[6] A.K. Barisal, N.C. Sahu, R.C. Prusty, and P.K. Hota, Short-term hydrothermal scheduling using gravitational search algorithm, *2012 2nd International Conf. on Power, Control and Embedded Systems*, Allahabad, India, 2012, 1–6.

[7] G.L. Decker and A.D. Brooks, Valve point loading of turbines, *Transactions of the American Institute of Electrical Engineers. Part III: Power Apparatus and Systems*, *77*(3), 1958, 481–484.

[8] M.I. Alomoush, Application of the stochastic fractal search algorithm and compromise programming to combined heat and power economic–emission dispatch, *Engineering Optimization*, 2019, 1–19.

[9] M. Saeedi, M. Moradi, M. Hosseini, A. Emamifar, and N. Ghadimi, Robust optimization based optimal chiller loading under cooling demand uncertainty, *Applied Thermal Engineering*, *148*, 2019, 1081–1091.

[10] N. Kumar, I. Hussain, B. Singh, and B.K. Panigrahi, Self-adaptive incremental conductance algorithm for swift and ripple-free maximum power harvesting from PV array, *IEEE Transactions on Industrial Informatics*, *14*(5), 2017, 2031–2041.

[11] N. Kumar, I. Hussain, B. Singh, and B.K. Panigrahi, Mppt in dynamic condition of partially shaded PV system by using WODE technique, *IEEE Transactions on Sustainable Energy*, *8*(3), 2017, 1204–1214.

[12] O. Abedinia, M. Zareinejad, M.H. Doranehgard, G. Fathi, and N. Ghadimi, Optimal offering and bidding strategies of renewable energy based large consumer using a novel hybrid robust-stochastic approach, *Journal of Cleaner Production*, *215*, 2019, 878–889.

[13] N. Ghadimi, A. Akbarimajd, H. Shayeghi, and O. Abedinia, Two stage forecast engine with feature selection technique and improved meta-heuristic algorithm for electricity load forecasting, *Energy*, *161*, 2018, 130–142.

[14] S. Mirjalili, S.M. Mirjalili, and A. Lewis, Grey wolf optimizer, *Advances in Engineering Software*, *69*, 2014, 46–61.

[15] K. Majumdar, P. Das, P.K. Roy, and S. Banerjee, Solving OPF problems using biogeography based and grey wolf optimization techniques, *International Journal of Energy Optimization and Engineering (IJEOE)*, *6*(3), 2017, 55–77.

[16] K. Zervoudakis and S. Tsafarakis, A mayfly optimization algorithm, *Computers & Industrial Engineering*, 106559(145), 2020.

[17] R. Eberhart and J. Kennedy, Particle swarm optimization, *Proceedings of the IEEE International Conference on Neural Networks*, vol. 4. Citeseer, 1995, 1942–1948.

[18] R.B. Goldberg, S.J. Barker, and L. Perez-Grau, Regulation of gene expression during plant embryogenesis, *Cell*, *56*(2), 1989, 149–160.

[19] M. Cornick, B. Hunt, E. Ott, H. Kurtuldu, and M.F. Schatz, State and parameter estimation of spatiotemporally chaotic systems illustrated by an application to Rayleigh–Bénard convection, *Chaos: An Interdisciplinary Journal of Nonlinear Science*, *19*(1), 2009, 013108.

[20] S.A. Gaganpreet Kaur, Chaotic whale optimization algorithm, *Journal of Computational Design and Engineering*, *5*, 2018, 275–284.

A. Appendix

Table A.1
A Comparative Study: MA versus CHMA-10 for Standard Test Bench Function

Function ID	**MA [16]**			**CHMA-10**		
	Min	Max	Ave	Min	Max	Ave
F1	6.54E-13	2.48E-06	1.18E-07	**4.32E-14**	7.48E-06	**8.21E-08**
F2	3.07E+01	2.16E+02	6.77E+01	**2.91E+01**	**1.86E+02**	**4.95E+01**
F3	1.97E-10	1.29E-04	7.39E-06	**1.81E-11**	2.36E-04	**6.25E-07**
F4	2.40E-56	8.55E-48	5.28E-49	**1.24E-58**	8.65E-48	**2.35E-51**
F5	−9.9999E-01	−9.9999E-01	−9.9999E-01	**−9.9999E-01**	**−9.9999E-01**	**−9.9999E-01**

Biographies

Kingsuk Majumdar received his M. Tech in Electrical Engineering from NIT, Durgapur, 2013. He is an assistant professor in the Department of Electrical Engineering, Dr. B C Roy Engineering College, Durgapur. His research interests include optimization, power system, power electronics, etc. He has guided several B. Tech and three M. Tech students. He is an associate member of The Institution of Engineers (India).

Provas K. Roy obtained Ph.D. degree in Electrical Engineering from National Institute of Technology Durgapur in 2011. He received his Master degree in Electrical Machine in 2001 from Jadavpur University. He finished his Engineering studies in Electrical Engineering from Regional Engineering College (presently known as National Institute of Technology) Durgapur. Presently, he is working as a professor in Electrical Engineering Department at Kalyani Government Engineering College, West Bengal, India. He was the recipient of the Outstanding Reviewer Award for IJEPES (Elsevier, 2018), EAAI (Elsevier, 2017), Renewable Energy Focus (Elsevier, 2018), ASEJ (Elsevier, 2017). He has published more than 150 research papers in National/International Journals and conference and more than 75 journals published in reputed SCI and Scopus indexed Journals, and more than 10 book chapters and two books of international standard. Six research scholars have obtained their Ph.D. degree under his guidance and 8 students are perusing their Ph.D. under his guidance. His research interest includes economic load dispatch, optimal power flow, FACTS, automatic generation control, radial distribution network, power system stabilizer, image processing, machine learning, evolutionary techniques, etc.

Subrata Banerjee received the Ph.D. degree in electrical engineering from IIT Kharagpur, Kharagpur, India, in 2005. He is currently a professor in the Department of Electrical Engineering, National Institute of Technology, Durgapur, India. He has successfully completed several research and consultancy projects, including one major from DST, Government of India. He has authored/coauthored about 180 research papers in national/international journals and conference records. He has filed three Indian patents and received one Indian Patent. He has guided nine Ph.D. and 21 M.Tech. students and many are pursuing their degree under his guidance. His research interests include power electronics converters, and application of control systems in power electronics and power systems. He is a Fellow of the Institution of Engineers, India, the Institution of Electronics and Telecommunication Engineers, India, and the Institution of Engineering and Technology, U.K. He was a recipient of several academic awards, including nine Best Paper Awards and the TATA RAO Prize. His biography is included in Marquis Whos Who 2007 and IBC Foremost Engineers of the World 2008. He is acting as an Associate Editor/Editorial Board in IEEE ACCESS, USA, and IET Power Electronics, U.K.